Pharmacogn. Res., 2024; 16(2):401-413.
https://www.phcogres.com

Original Article

Protective Effects of *Vaccinium arctostaphylos* L. against Oxymetholone-Injured Liver and Kidney Injury in BALB/c Mice: An Integrated Biochemical, Stereological, Histopathological, and Immunohistochemical Study

Elnaz Khordad[1], Mohsen Akbaribazm[2,3,*], Seyed Moein Hosseini[4], Yasaman Rahmani[4]

[1]Department of Anatomical Sciences, School of Medicine, Torbat Heydariyeh University of Medical Sciences, Torbat Heydariyeh, IRAN.
[2]Department of Anatomy, Torbat Heidariyeh University of Medical Sciences, Torbat Heidariyeh, IRAN.
[3]Department of Basic Medical Sciences, Khoy University of Medical Sciences, Khoy, IRAN.
[4]Student Research Committee, Torbat Heydariyeh University of Medical Sciences, Torbat Heydariyeh, IRAN.

ABSTRACT

Background: Anabolic steroids, like Oxymetholone (OM), can imitate testosterone and cause harm to the liver and kidneys. **Objectives:** In this study, the ameliorative effects of *Vaccinium arctostaphylos* L. (*V. arctostaphylos*) on OM-induced liver and kidney damage were investigated using various methods. **Materials and Methods:** BALB/c mice (Thirty-six in 6 group/6 mice) were included as sham, OM, three OM groups treated with different doses of *V. arctostaphylos* fruit extract (OM+100, OM+200, and OM+400 *V. arctostaphylos*), and a group solely treated with 400 *V. arctostaphylos*. Blood samples collected on the 51st day assessed biochemical parameters and oxidative stress factors in the liver and kidney. Stereological and histopathological analyses were conducted using isolated liver and kidney tissues, while immunohistochemistry measured apoptosis levels using p53 and Bcl-2 positive cells. **Results:** The results indicated that *V. arctostaphylos* fruit extract protected the liver and kidney from OM-induced damage and maintained their normal function. Liver enzyme levels and kidney functional parameters were close to normal, and SOD and GPx activity increased while NO levels decreased. Stereological analysis showed that *V. arctostaphylos* preserved the normal structure of the liver and kidney and reduced the p53 positive cells while increasing Bcl-2 cell count. **Conclusion:** These findings suggest that *V. arctostaphylos* fruit extract, rich in polyphenols and possessing antioxidant properties, can enhance protection against OM-induced hepato-renal oxidative damage.

Keywords: *Vaccinium arctostaphylos* L., Kidney, Liver, Oxymetholone.

Correspondence:
Dr. Mohsen Akbaribazm
Department of Anatomy, Torbat Heidariyeh University of Medical Sciences, Torbat Heidariyeh, IRAN.
Department of Basic Medical Sciences, Khoy University of Medical Sciences, Khoy, IRAN.
Email: akbarim3@thums.ac.ir; akbarimohsen64@gmail.com
ORCID ID: 0000-0001-9162-8706.

Received: 17-10-2023;
Revised: 21-12-2023;
Accepted: 16-02-2024.

INTRODUCTION

Oxymetholone (OM) is classified as an Anabolic Androgenic Steroid (AAS) and a testosterone analogue, known to elicit a range of adverse effects. These effects include hepatoadenoma, amenorrhea, gynecomastia, hepatitis, elevated cholesterol levels, cholestasis, liver cancer, and kidney and liver toxicity, even at therapeutic doses (<5 mg/kg).[1] The hepatic metabolism of OM involves processes such as reduction at the C3 position, hydroxylation at the C17 position, and oxidation at the C2 position, which contribute to hepatic damage. This damage manifests as hepatocyte destruction and liver fibrosis, primarily due to the production of metabolites like mestanolone (17α-methyl-dihydrotestosterone).[2] Moreover, the administration of OM leads to the generation of Reactive Oxygen Species (ROS), which can cause tissue damage and disrupt the physiological functioning of vital organs like the heart, liver, kidneys, testes, and central nervous system.[3] In a study conducted on BALB/c mice, a daily dose of 5 mg/kg of OM resulted in increased oxidation of parenchymal cell membranes and decreased serum catalase activity over a 30-day period.[4] Further evidence suggests that OM can elevate liver enzyme levels, including ALT, ALP, and AST, in male bodybuilders, leading to heightened hepatocyte apoptosis and impaired liver function. This increased ROS production associated with OM usage can also elevate pro-inflammatory cytokine levels, trigger lymphocyte infiltration, and induce inflammatory foci in liver tissue.[5]

Oxymetholone (OM) has the potential to induce rhabdomyolysis, which can lead to acute renal failure by elevating levels of creatinine

DOI: 10.5530/pres.16.2.50

phosphokinase and lactate dehydrogenase. By disrupting renal homeostasis and hemodynamics, increasing blood pressure, and upregulating apoptotic genes and caspase-dependent apoptotic pathways, OM interferes with the normal physiological activity of the kidneys, ultimately contributing to the development of chronic kidney disease.[6] Additionally, OM has been found to increase the levels of pro-inflammatory cytokines, including Interleukin-1β (IL-1β), Tumor Necrosis Factor α (TNF-α), and IL-6, through the elevation of Reactive Oxygen Species (ROS) and testosterone levels.[7] These cytokines can contribute to the destruction of the Distal Convoluted Tubules (DCT) and Proximal Convoluted Tubules (PCT), leading to tubule-interstitial fibrosis.[8] Moreover, the severe oxidative stress induced by OM is associated with immune alterations, contributing to various diseases. While numerous studies have focused on investigating individual compounds to mitigate the side effects of Anabolic Androgenic Steroids (AAS) on different organs, particularly the liver and kidneys, certain plants containing polyphenolic compounds, such as flavonoids and isoflavones, have shown promise in regulating ROS, interacting with androgen and estrogen receptors, and counteracting secondary metabolites of AAS in long-term and non-therapeutic doses. These plant compounds can provide protection to hepatic parenchymal cells (hepatocytes) and renal parenchymal cells against AAS-induced damage by targeting various apoptotic and inflammatory signaling pathways.[9,10]

Vaccinium arctostaphylos L. a member of the Ericaceae family, is characterized by its heart-shaped leaves with toothed edges and is commonly found in the northern and northwestern regions of Iran, including Ardebil, Tabriz, Astara, and Mazandaran.[11] Phytochemical studies utilizing LC-ESI/MS (liquid chromatography electrospray ionization mass spectrometry) have revealed that the fruit extract of *V. arctostaphylos* is rich in isoflavonoids, such as Genistein, Daidzein, Glycitein, Biochanin A, Formononetin, Puerarin, Coumestrol, and delphinidin. It also contains flavonoids like Quercetin, Kaempferol, Apigenin, Petunidin, p-coumaric acid, Myricetin, Hesperetin, Naringenin, Rutin, Catechin, Epicatechin, Epigallocatechin, and malvidin.[12] These compounds, including flavonoids, isoflavonoids, and anthocyanins, have the potential to modulate the activity of apoptotic proteins (such as Bcl2, TRAF1, and Survivin) and cell cycle-regulating proteins (like Cyclin D) through pathways like NF-κB/MAPK and PI3K/Akt/mTOR. Additionally, their antioxidant and anti-inflammatory properties have been shown to enhance the body's natural anti-inflammatory/antioxidant system, protecting cells from oxidative stress.[13,14] A study conducted by Hakimi *et al.* (2014) on 46 patients with high blood pressure and hyperlipidemia revealed that *V. arctostaphylos* fruit extract, administered in capsule form at a dosage of 500 mg, significantly reduced serum levels of inflammatory factors, including IL-6, TNF-α, ICAM-1, and VCAM-1, compared to the placebo and control groups.[15] Furthermore, Feshani *et al.* (2011) investigated the anti-diabetic properties of the fruit extract and observed that it effectively lowered blood sugar and triglyceride levels while enhancing antioxidant parameters such as catalase enzyme activity, Superoxide Dismutase (SOD), and Glutathione Peroxidase (GPx) in rats.[11]

In light of this, the protective effects of *V. arctostaphylos* fruit were assessed in relation to hepatorenal damage induced by OM using biochemical, stereological, histopathological, and immunohistochemical analysis.

MATERIALS AND METHODS

V. arctostaphylos fruit extract preparation

The *V. arctostaphylos* fruit extract was obtained by grinding 2000 g of dried fruit into a powder using a soil grinder (model number: SA-45F; GlobalGilson company, US). The resulting powder was mixed with a solution of water and ethanol in a ratio of 30:70 v:v and left to incubate in a dark room at a temperature of 25-30°C for a period of 72 hr. After the incubation period, the mixture was filtered through a paper filter (size number: 42; Millipore, US) and concentrated using a rotary evaporator (Asynt Ltd., Headquarters, United Kingdom). The final yield of the *V. arctostaphylos* fruit extract was 20% (equivalent to 150 g) and it was stored at a temperature of -20°C.[16]

Animals and experimental design

In this study, a total of 36 BALB/c mice weighing 25±5 g each were enrolled, and they were divided into 6 groups with 6 mice per group (n=6/group), as indicated in Table 1. Before the initiation of the study, a 3-day adaptation period was provided to allow the mice to acclimate to their surroundings and cages. The mice were housed under standardized conditions at a temperature of 23±2°C, a humidity level of 45±5%, and a 12/12 light/dark cycle. Throughout the entire study, the mice had unrestricted access to drinking water and were fed standard laboratory animal pellets. According to the manufacturer's instructions, the standard pellets (per 100 g) consist of 4 Mcal energy, 20 g of total fat, 24 g of total protein, and 25 g of carbohydrates. Additionally, the pellets contain various micronutrients, such as 0.9 g of calcium, 0.6 g of phosphorus, 0.4 g of iron, 0.5 g of magnesium, and 0.1 g of cobalt. The fatty acid composition of the pellets includes 250 mg of palmitic acid, 350 mg of arachidonic acid, and 400 mg of linoleic acid. All procedures adhered to international standard guidelines and protocols and were approved by the ethics committee of the (Torbat Heydarieh University of Medical Sciences) with the approval number (IR.THUMS.AEC.1401.006).

Group 1: Sham group: Mice were administered 0.1 cc (100 µL) of Distilled Water (DW) per day via gavage for duration of 50 days.

Group 2: Oxymetholone group (OM): Mice were given 5 mg/kg of OM dissolved in 500 µL of DW on days 10, 20, 30, and 40 via gavage.

Groups 3, 4, and 5: OM in combination with *V. arctostaphylos* fruit extract treatment groups (OM+100, 200, and 400 *V. arctostaphylos*): Mice received 5 mg/kg of OM dissolved in 500 µL of DW on days 10, 20, 30, and 40 via gavage, along with 100, 200, and 400 mg/kg of *V. arctostaphylos* fruit extract via gavage for a duration of 50 days.

Group 6: 400 mg/kg *V. arctostaphylos* fruit extract treatment group (400 *V. arctostaphylos*): Mice were administered 400 mg/kg of *V. arctostaphylos* fruit extract via gavage for duration of 50 days.

During the study, OM (on days 10, 20, 30, and 40) and *V. arctostaphylos* fruit extract (administered consecutively for 50 days) were orally administered at specific times of the day (9 am and 3 pm, respectively). The LD_{50}, pilot study, and previous research were utilized to determine the optimal dose that would be both effective and non-toxic.[17,4]

Acute toxicity test (LD_{50}) of *V. arctostaphylos* fruit extract

Lork's two-step method was implemented to assess the LD_{50} (lethal dose for 50% of tested subjects) of the *V. arctostaphylos* fruit extract. This approach relies on measuring the toxicity of the extracts using animal models. Initially, 9 BALB/c mice were divided into 3 groups and administered doses of 10, 100, and 1000 mg/kg of *V. arctostaphylos* fruit extract. Subsequently, the mice were monitored for a 24 hr period, noting any toxic effects or potential fatalities within the respective groups. Following this, 3 BALB/c mice received doses of 30, 300, and 3000 mg/kg of the same extract, with their health and potential fatalities again closely observed for 24 hr. The minimal Dose (D_m) at which toxic effects (such as anorexia, significant weight loss, nausea, and diarrhea) or death occurred, as well as the highest dose (D_h) without any observed signs of toxicity or mortality, were then recorded for use in the LD_{50} calculation (Formula 1).[18]

$$LD_{50} = \sqrt{Dm \times Dh}$$

Formula 1. LD_{50} based on Lork's method.

V. arctostaphylos fruit extract Total Phenolic Content (TPC)

To determine the Total Phenolic Content (TPC), the modified Folin-Ciocalteu method, utilizing gallic acid as the reference compound, was employed. In this procedure, a mixture consisting of carbonate solution (7.5%, 0.8 mL), Folin-Ciocalteu reagent (2 mL), and *dry V. arctostaphylos* fruit extract (500 mg) were incubated at 37°C for 90 min. Following this, gallic acid standards with concentrations ranging from 50 to 400 µg/mL were added to the mixture, followed by another incubation at 37°C for 60 min. The absorbance of the resulting mixture was then measured at 765 nm using a UV-1280 Shimadzu spectrophotometer (Shimadzu, Japan).[19]

V. arctostaphylos fruit extract Total Flavonoid Content (TFC)

To determine the Total Flavonoid Content (TFC), the modified Miliauskas method, using rutin as the reference compound, was employed. In this procedure, a mixture consisting of aluminum trichloride solution (20 mg/mL, 1 mL), potassium acetate solution (1 M, 0.1 mL), and dry *V. arctostaphylos* fruit extract (500 mg) was incubated at 37°C for 60 min. Following this, rutin standards with concentrations ranging from 0.025 to 0.075 mg/mL were added to the mixture, followed by another incubation at 37°C for 40 min. The absorbance of the resulting mixture was then measured at 415 nm using a UV-1280 Shimadzu spectrophotometer (Shimadzu, Japan).[19]

V. arctostaphylos fruit extract 2, 2-diphenyl-1-picrylhydrazyl (DPPH) radical scavenging activity

In this study, the modified Brand and Williams method was utilized to measure the DPPH (2,2-diphenyl-1-picrylhydrazyl) radical scavenging activity, expressed in µmol Trolox equivalent. The procedure involved the preparation of a solution comprising 60 µM of DPPH radical, 3.5 mL of Distilled Water (DW), and serial dilutions of hydroalcoholic *V. arctostaphylos* fruit extract (ranging from 0.025 to 0.150 mg/mL). This mixture was then incubated at 25°C for 60 min. Subsequently, the absorbance of the resulting mixture was measured at 515 nm using a UV-1280 Shimadzu spectrophotometer (Shimadzu, Japan).[19]

V. arctostaphylos fruit extract ferric reducing antioxidant power (FRAP) levels

In this study, the modified Benzie and Strain calorimetric method was employed to assess the total antioxidant capacity

Table 1: Group's.

Groups	Treatment with administration rout	Period of administration
Sham	100 µL of D.W./ p.o.	50 days
OM	5 mg/kg OM dissolved in 500 µL of D.W./gavage	Days 10, 20, 30, and 40.
OM+100 *V. arctostaphylos*	OM+100 mg/kg *V. arctostaphylos*/fifty consecutive days	Fifty consecutive days.
OM+200 *V. arctostaphylos*	OM+200 mg/kg *V. arctostaphylos*/fifty consecutive days	Fifty consecutive days.
OM+400 *V. arctostaphylos*	OM+400 mg/kg *V. arctostaphylos*/fifty consecutive days.	Fifty consecutive days.
400 *V. arctostaphylos*	400 mg/kg *V. arctostaphylos*/fifty consecutive days.	Fifty consecutive days.

of *V. arctostaphylos* fruit extract. This method relies on the measurement of Ferric Reducing Antioxidant Power (FRAP), where the conversion of yellow-colored Fe (III)-2,4,6-Tris(2-p yridyl)-s-triazine (TPTZ) to blue-colored Fe (II)-TPTZ indicates the presence of antioxidant activity. The procedure involved mixing a solution comprising 40 mM of TPTZ (1 mL), FRAP solution (3 µL), and 50 µL of hydroalcoholic *V. arctostaphylos* fruit extract. The resulting mixture was then incubated at 37°C for 15 min. Subsequently, the mixture underwent centrifugation (15,000 g for 10 min), and the absorbance was measured at 593 nm using a UV-1280 Shimadzu spectrophotometer (Shimadzu, Japan).[4]

Liver and kidney serum related biochemical parameters

On day 51, at the conclusion of the study, after administering pre-anesthesia using ketamine and xylazine with 80 and 100 mg/kg respectively, blood samples were collected from the heart to assess the functional levels of serum biochemical factors associated with the liver and kidneys. The serum levels of Alanine aminotransferase (ALT), Alkaline Phosphatase (ALP), Aspartate aminotransferase (AST), Total Protein (TP), albumin (ALB), Bilirubin (BIL), Blood Urea Nitrogen (BUN), and Creatinine (Cr) were evaluated. This assessment was performed using an autoanalyzer (ChemWell T-4620 biochemistry autoanalyzer, Tehran, Iran).

Nitric Oxide (NO) assay

In this study, the Griess method was employed to quantify the levels of Nitric Oxide (NO) in serum samples. The procedure involved combining 500 mL of serum samples with 6 mg of zinc oxide and 500 µL of Griess solution. The resulting mixture was subjected to centrifugation at 10,000 g for 15 min and then incubated at 37°C for 60 min. Subsequently, the absorbance of the mixture was measured at 540 nm and 630 nm using a UV-1280 Shimadzu spectrophotometer (Shimadzu, Japan).[4]

Serum endogenous enzymes antioxidant activity

The serum activity of SOD (catalog number: E-EL-R1424) and GPx (catalog number: E-EL-R2491) was assessed using a commercially available ELISA kit (Elabscience, United States) following the manufacturer's instructions.[20]

Liver and kidney stereology assay

In this study, the liver and kidney samples were isolated on the 51st day to determine their primary and final volumes. The initial volume was measured using the immersion method, while Cavalieri's principle was applied to calculate the final volume, accounting for tissue shrinkage. The primary volume of each tissue was determined by immersing the samples in DW and measuring the difference in volume. Isotropic Uniform Random (IUR) sections were prepared using the Orientator method. The samples were divided into circles, and random numbers were used to make cuts. The resulting slices were further divided into 2 mm sections. From each slice, 6-8 sections were randomly selected for analysis. Tissue shrinkage was calculated by measuring the diameter of a circular punch taken from one of the sections (formula 2). The selected sections underwent standard tissue passage steps, followed by paraffin molding and slicing with a rotary microtome to achieve a diameter of 5 µm. The final diameter of the circular section was measured after completion of the tissue passage steps and used in subsequent calculations.

$$\text{Shrinkage} = 1 - \sqrt{R1/R2}$$

Formula 2: Tissue shrinkage. R1: Diameter of punched sample before tissue passage and R2: Diameter of punched sample after tissue passage.

Periodic Acid Schiff (PAS) and Hematoxylin and Eosin (H and E) staining were used to evaluate stereological parameters in liver and kidney, respectively. To calculate the relative volume of structures within each tissue, we utilized a point probe. This probe consisted of a 10×10 transfer screen with 50 points displayed on the monitor. The number of points situated on each structure within the field of view was then tallied and employed with formula 3. This method allowed us to derive the relative volume for each individual structure.

$$Vv = \Sigma P\,\text{structure}/\Sigma P\,\text{reference}$$

Formula 3: Volume density (V_v). ΣP structure: The number of points located on each structure and ΣP reference: total number of points (50 point) (Figure 1A).

o calculates the ultimate size of each structure; we multiplied the proportional volume of each structure by the reference volume. The reference volume was derived by subtracting the shrinkage amount from the final volume (Formula 4).

$$V\,\text{structure} = Vv \times \text{final volume of liver or kidney}$$

Formula 4: Final volume of each structure.

The physical dissector method was utilized to determine the quantity of glomeruli in each kidney. This involved conducting a pair of cuts, 350 µm apart, in each kidney. Specifically, the first cut (reference) and the seventh cut (control) were considered. Two frame probes, possessing an identical area of 900 μm^2, were placed on separate monitors, employing the same software system and camera. The glomeruli were tallied based on their presence within the frame probe, their intersection with the left or right side, or their intersection with the top or bottom side. Any glomeruli observed solely in the reference section (seventh section) were not included in the count. Once 100 glomeruli were counted and the dissector height was calculated (30 µm), the data was formulated into the provided equation (formula 5) to compute the numerical density of glomeruli (Figure 1B).

$$Nv = \Sigma Q / a(\text{frame}) \times h \times \Sigma P$$

Formula 5: Numerical density (N_v). ΣQ: The total number of glomeruli counted (100 glomeruli in each kidney), a (frame) is the area of the dissector frame (900 μm^2), h is the height of the dissector (30 μm) and ΣP is the number of frames counted in each kidney.

$$N\,\text{glomeruli} = Nv \times \text{final volume of kidney}$$

Formula 6: Total number of glomeruli.

Finally, after calculating the numerical density, the resulting number was multiplied by the total volume and the number of glomeruli was determined (Formula 6).[21,22]

Immunohistochemistry (IHC) assay

In order to assess the anti-apoptotic effects of *V. arctostaphylos* fruit extract on liver and kidney tissues exposed to OM toxicity, we utilized the quantification of p53 and Bcl-2 positive cells. Initially, tissue slices with a thickness of 5 μm were prepared using a rotary microtome (model number: RM2125 RTS, Leica Biosystems, United States). Subsequently, the slides underwent 60 min incubation at 95°C and were treated with 100 μL of 3% H2O2, followed by a 40 min re-incubation at 37°C. 1:400; HRP complex (200 μL) was applied to the slides, followed by incubation with chromogen 3,3'-diaminobenzidine (200 μL) at 25°C. Throughout the procedure, 5% bovine serum albumin served as the blocking solution, and 1X PBS was used as the washing buffer. Finally, an Olympus optical microscope (IX71) connected to a Kecam was used to examine a total of 10 fields of view at 400× magnification (with using ver. 3.7 Top-View software). The number of p53 and Bcl-2 positive cells was quantified, and their respective ratios to total cells (%) were reported.[16]

Histopathological assay

Similar to the instructions provided in the "stereology assay" section, the tissues were fixed in 10% formalin for 72 hr and subsequently prepared as paraffin blocks using L-shaped molds. 5 μm sections were then obtained from the blocks and subjected to routine histological procedures. Liver tissue samples were stained with H and E, while kidney samples were stained using PAS and Jones' Methenamine Silver stain. Finally, an Olympus optical microscope (IX71) connected to a Kecam was used to examine a total of 10 fields of view at 400×magnification (with using ver. 3.7 Top-View software).[21]

Statistical Analysis

Or graph creation, we utilized GraphPad Prism software version 8. To compare the mean differences between groups in the statistical analysis, we employed ver. XVI SPSS software. The normality between groups was assessed using the Kolmogorov-Smirnov test with $p>0.05$ and followed by conducting a one-way Analysis of Variance (ANOVA) test and Tukey's post hoc test. A significance level of $p<0.05$ was considered statistically significant, and all data were presented as mean±Standard Deviation (SD).

RESULTS

TPC, TFC, DPPH, and FRAP of *V. arctostaphylos* fruits extract

The analysis of *V. arctostaphylos* fruit extract revealed that it contained 229.4±10.7 mg GAE/g dried extract of TPC and

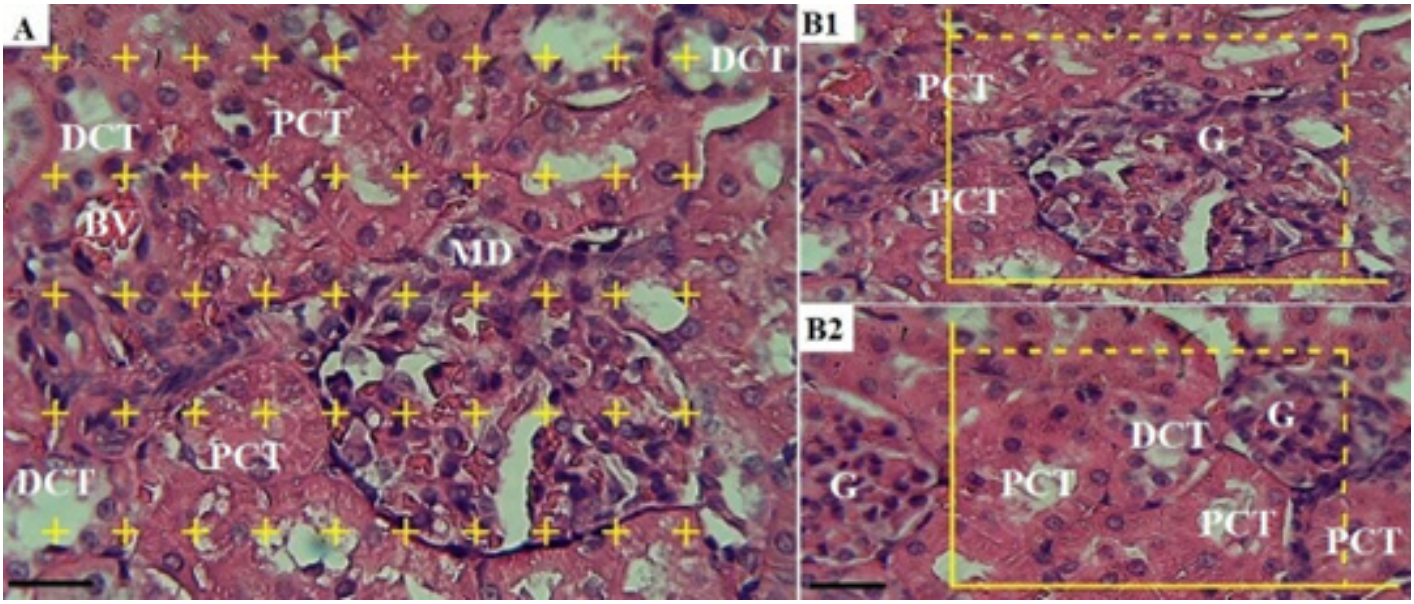

Figure 1: (a) Using point probe to calculate the volumetric density of liver and kidney tissue substructures. (B1 and B2) Using framework probe to calculate the numerical density of kidney glomeruli (H and E×400, scale bar=25 μm). Normal Glomerulus (G), Proximal Convoluted Tubule (PCT), Distal Convoluted Tubule (DCT), Blood Vessel (BV), and Macula Densa (MD).

120.9±11.7 mg RUE/g dried extract of TFC. Furthermore, the extract exhibited strong antioxidant properties and demonstrated a total antioxidant capacity. Specifically, its DPPH free radical scavenging level was measured at 519.1±10.1 µmol eq. Trolox/10 g dried extract, while its FRAP content was recorded at 1516.6±55.1 mmol Fe^{+2} mg dried extract (Table 2).

LD_{50} of *V. arctostaphylos* fruit extract

After conducting a 24 hr monitoring of the groups and carefully recording toxic symptoms and potential deaths, it was observed that mice treated with a dose of 3000 mg/kg of *V. arctostaphylos* fruit extract experienced adverse effects, including nausea, anorexia, and weight loss. However, no fatalities were reported within this group. Thus, applying Lork's two-step method, the determined values were D_m (3000 mg/kg) and D_h (1000 mg/kg). By applying the relevant formula of this method, the LD_{50} (lethal dose, 50%) of the *V. arctostaphylos* fruit extract was calculated to be 1.732 g/kg. it can be concluded that doses below 1732 mg/kg of this fruit extract are considered non-toxic to mice, making them suitable for further research purposes.

Mice Body (BW), Liver (LW) and Kidney Weights (KW)

The evaluation of the mice weight parameters revealed significant differences when comparing the effects of sham and OM. OM resulted in a significant decrease (p<0.05) in Body Weight (BW), while there was a significant increase (p<0.05) in Liver Weight (LW) and Kidney Weight (KW) in mice. On the other hand, *V. arctostaphylos* showed a dose-dependent improvement in weight parameters. Specifically, in the OM+400 *V. arctostaphylos* group where a dose of 400 fruit extracts was administered, significant changes (p<0.05) were observed. These changes led to an increase in BW and a decrease in LW and KW compared to the OM group (Figure 2).

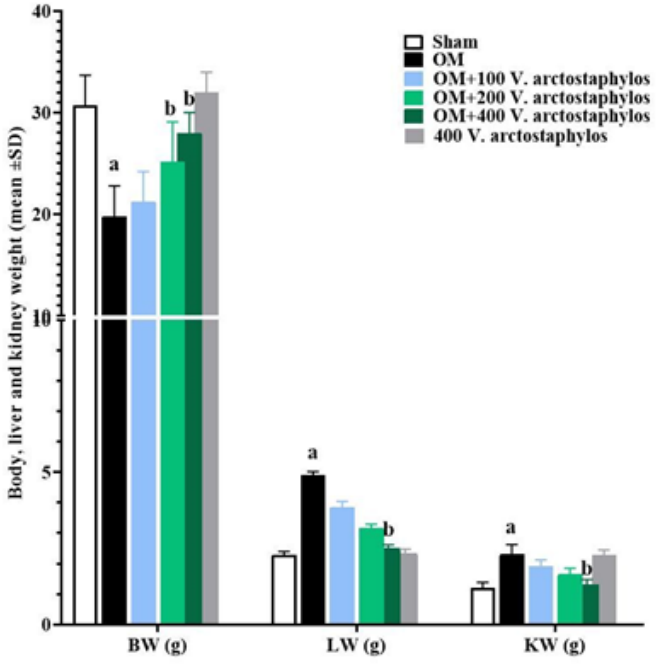

Figure 2: Total body (BW) (g), liver (LW) (g), and kidney weights (KW) (g) in experimental groups (means±SD).[a] (p<0.05) sham *vs.* OM groups and[b] (p<0.05) OM *vs. V. arctostaphylos* treated groups.

Liver and kidney serum related biochemical parameters

After analyzing the biochemical data concerning liver and kidney function, noteworthy findings emerged. It was observed that OM resulted in a significant increase (p<0.05) in Bilirubin (BIL) and liver enzymes when compared to the sham group. Additionally, the OM group displayed a significant decrease (p<0.05) in Total Protein (TP) and Albumin (ALB), in contrast to the sham group. However, *V. arctostaphylos* fruit extract demonstrated a positive impact on the liver's biochemical function in a dose-dependent manner. Specifically, the administration of 200 and 400 mg/kg of this plant's fruit extract (in the OM+ 200 and 400 *V. arctostaphylos* groups) yielded significant reductions (p<0.05) in liver enzyme activity and BIL levels. Furthermore, these groups experienced a notable decrease in ALB and TP levels compared to the OM group (p<0.05) (Figure 3).

Furthermore, OM supplementation resulted in a significant increase (p<0.05) in Blood Urea Nitrogen (BUN) and Creatinine (Cr) compared to the sham group. However, *V. arctostaphylos* exhibited the ability to significantly reduce (p<0.05) both kidney functional indices at doses of 200 and 400 mg/kg (in the OM+200 and 400 *V. arctostaphylos* groups) when compared to the OM group (Figure 4A).

Serum NO levels and GPx and SOD activities

By inducing the generation of Reactive Oxygen Species (ROS), OM exhibited a significant increase (p<0.05) in serum Nitric Oxide (NO) levels compared to the sham group. Moreover, it caused a noteworthy reduction (p<0.05) in the activity of both enzymes when compared to the sham group. The findings clearly indicate that *V. arctostaphylos* in the OM+200 and 400 *V. arctostaphylos* groups, due to its strong antioxidant capacity, demonstrated a significant decrease in serum NO levels and a substantial improvement (p<0.05) in the serum activity of both

Table 2: *V. arctostaphylos* extract DPPH, FRAP, TPC, and TFC level.

V. arctostaphylos extract parameters/Unit	Value*
Total phenolic content[a]	229.4±10.7
Total flavonoid content[b]	120.9±11.7
DPPH[c]	519.1±10.1
FRAP[d]	1516.6±55.1

*Mean±SD (n=3);[a] (mg GAE/ g dried extract),[b] (mg RUE/ g dried extract),[c] (µmol eq. Trolox/10 g dried extract), and[d] (mmol Fe^{+2}mg dried extract).

Table 3: The mean individual volume (10^{-4} mm³), total volume (mm³), and total number of glomeruli in experimental groups (mean±SD).[a] ($p<0.05$) sham *vs.* OM groups and[b] ($p<0.05$) OM *vs. V. arctostaphylos* treated groups.

Groups	Total volume (mm³)	Total number	Mean individual volume (10^{-5} mm³)
Sham	8.2±0.4	10221±954	15.11±1.2
OM	15.3±1.2[a]	6591±811[a]	32.4±3.2[a]
OM+100 *V. arctostaphylos*	13.6±0.8	7219±620	25.1±1.2
OM+200 *V. arctostaphylos*	11.2±0.7	8911±825	20.6±0.9
OM+400 *V. arctostaphylos*	9.1±0.5[b]	9624±658[b]	16.9±0.7[b]
400 *V. arctostaphylos*	8.4±0.7	11021±511	15.7±4.4

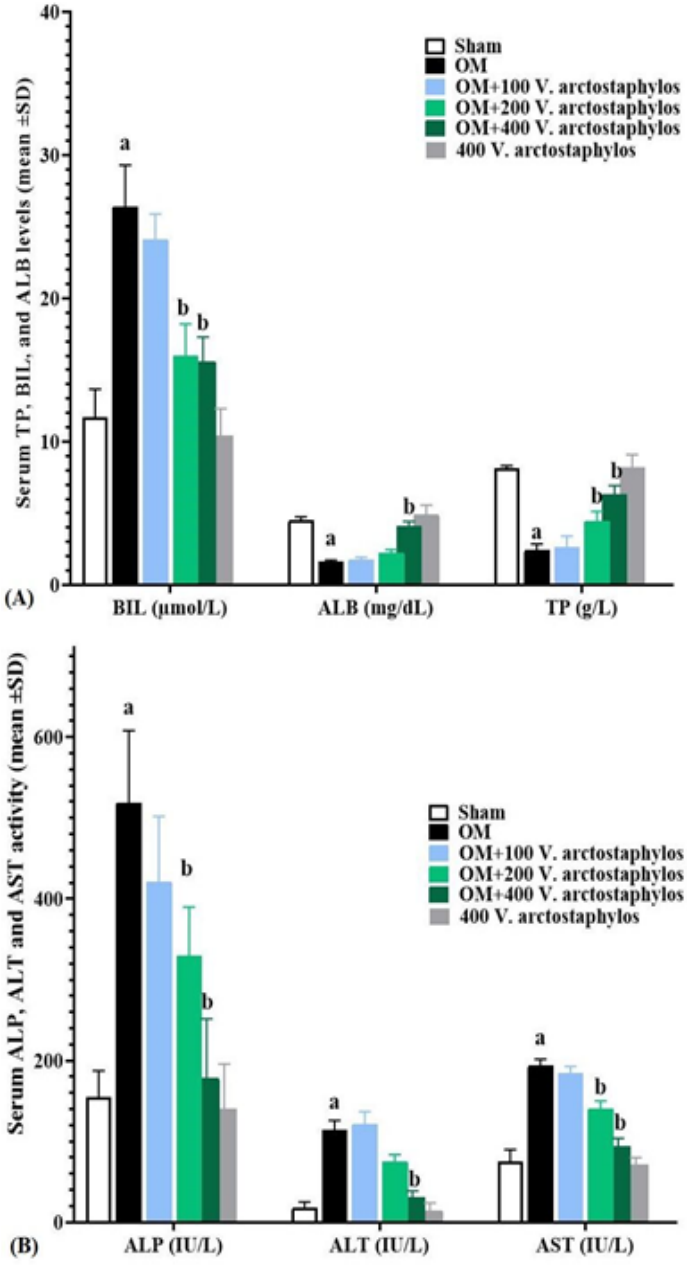

Figure 3: (A) Serum levels of Bilirubin (BIL) (µmol/L), Albumin (ALB) (mg/dL), and Total Protein (TP) (g/l). (B) Serum Aspartate Aminotransferase (AST), Alanine Aminotransferase (ALT), and Alkaline Phosphatase (ALP) (IU/l) enzymes activity in experimental groups (means±SD).[a] ($p<0.05$) sham *vs.* OM groups and[b] ($p<0.05$) OM *vs. V. arctostaphylos* treated groups.

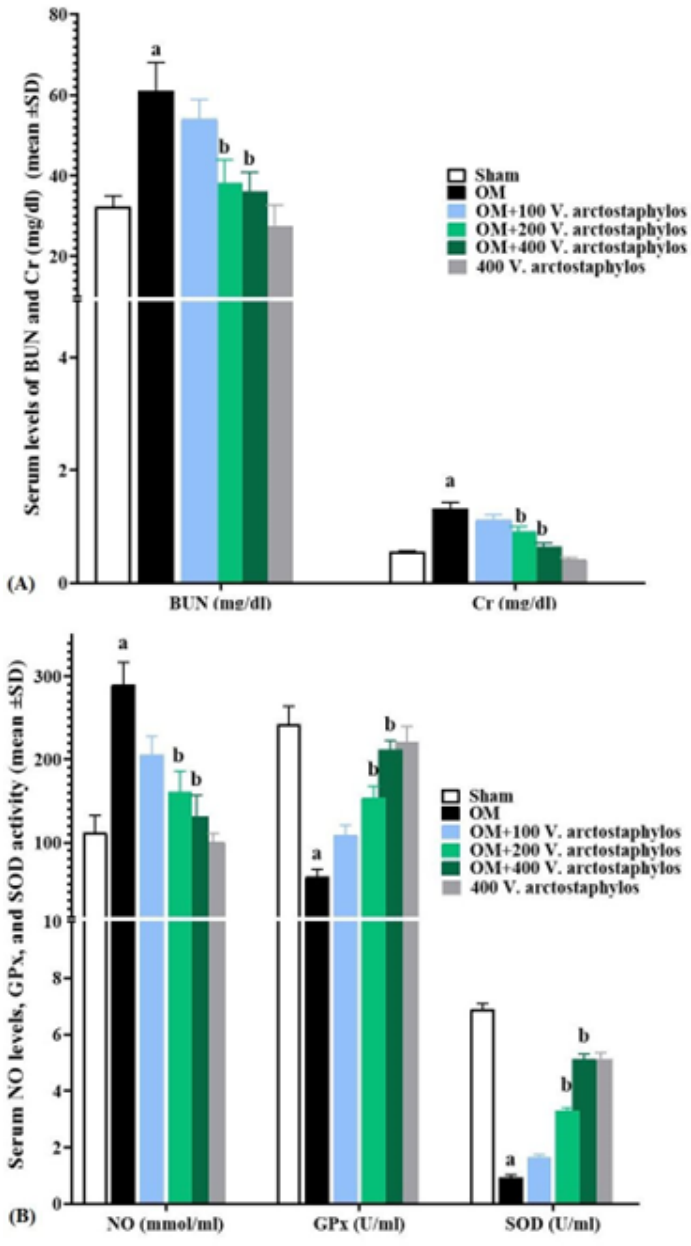

Figure 4: (A) Serum levels of Blood Urea Nitrogen (BUN) and Creatinine (Cr) (mg/dL). (B) Serum levels of Nitric Oxide (NO) (mmol/mL) alongside Superoxide Dismutase (SOD) and Glutathione Peroxidase (GPx) (IU/l) enzymes activity in experimental groups (means±SD).[a] ($p<0.05$) sham *vs.* OM groups and[b] ($p<0.05$) OM *vs. V. arctostaphylos* treated groups.

endogenous antioxidant enzymes when compared to the OM group (Figure 4B).

Liver and kidney stereology results

The data concerning kidney stereological parameters revealed that the administration of OM resulted in severe structural alterations in the kidneys. Compared to the sham group, the kidneys exhibited a significant decrease (p<0.05) in their final Volume (KV), accompanied by a noteworthy reduction (p<0.05) in the volumes of renal tubules, including Proximal Convoluted Tubules (PCT), Distal Convoluted Tubules (DCT), Loop of Henle (LHV), and Collecting Tubules (CT). Conversely, there was a significant increase (p<0.05) in the volume of Vessels (RV) and interstitial tissue (RI). These findings suggest that connective tissue, in the form of scars and fibrosis, replaces the primary parenchyma (tubular parenchyma), ultimately leading to impairment in the functional units of the kidneys. However, the administration of *V. arctostaphylos* fruit extract exhibited a dose-dependent improvement in the normal structure of the kidneys. Notably, a dose of 400 mg/kg (in the OM+400 *V. arctostaphylos* group) significantly increased (p<0.05) the final volume of the kidney and renal tubular parenchyma (PCT, DCT, LHV, and CT) while decreasing (p<0.05) the RV and RI in comparison to the OM group (Figure 5).

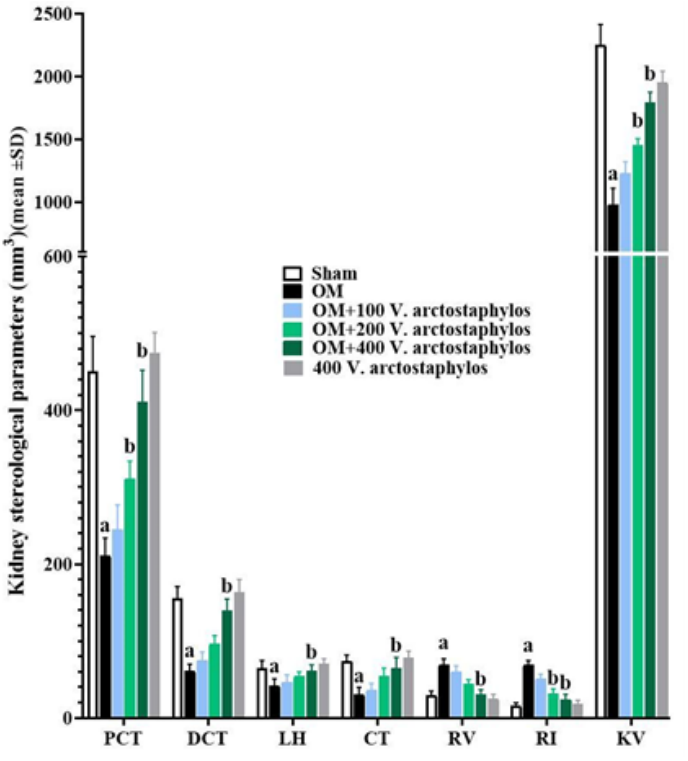

Figure 5: Volume of Proximal Convoluted Tubules (PCT), Distal Convoluted Tubules (DCT), Loop of Henle (LHV), Collecting Tubules (CT), Vessels (RV), Interstitial tissue (RI) and Kidney (KV) (mm³) in experimental groups (means±SD).[a] (p<0.05) sham *vs.* OM groups and[b] (p<0.05) OM *vs. V. arctostaphylos* treated groups.

Regarding the indicators related to glomeruli within the studied groups, OM significantly increased (p<0.05) the total volume and mean individual volume while decreasing (p<0.05) the total number of glomeruli compared to the sham group. However, *V. arctostaphylos* fruit extract exhibited a dose-dependent decrease (p<0.05) in the total and mean individual volumes of the glomeruli while increasing (p<0.05) the total number of glomeruli. Remarkably, these changes were significant in the 400 mg/kg dosage (in the OM+400 *V. arctostaphylos* group) when compared to the OM group (Table 3).

The stereology indicators related to the liver also demonstrated structural modifications caused by OM. It significantly increased (p<0.05) the volume indicators of the liver, including the liver portal triad (HP), Bile Duct (BD), vessels (BA), interstitial tissue (BI), and Liver (LV), while resulting in a significant decrease (p<0.05) in the volume of active and functional liver parenchyma represented by the volume of Hepatocytes (HC) compared to the sham group. However, the administration of *V. arctostaphylos* fruit extract exerted protective effects on the liver's normal structure against the oxidative changes induced by OM in a dose-dependent manner. Notably, a dosage of 400 mg/kg led to a significant decrease (p<0.05) in the volume indicators of the liver (HP, BD, BA, BI, and LV) and a significant increase (p<0.05) in the HC compared to the OM group (Figure 6).

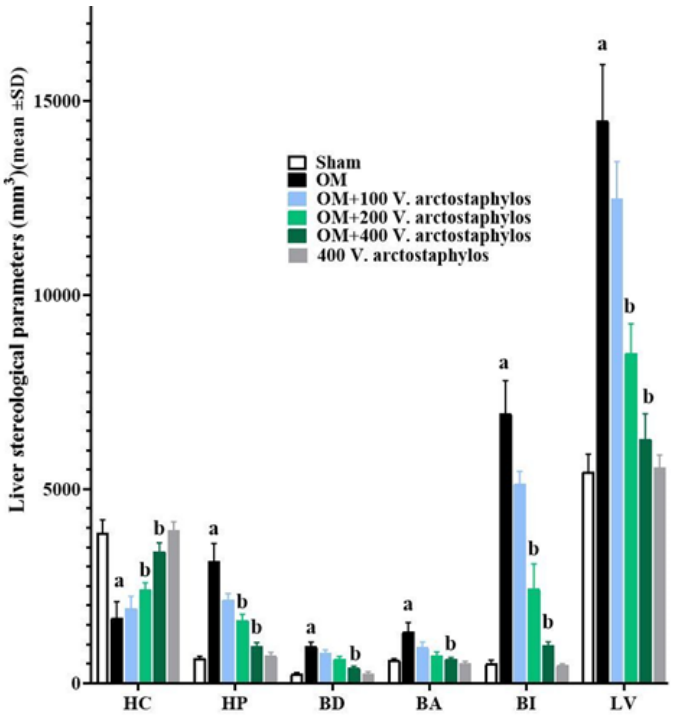

Figure 6: Volume of Hepatocytes (HC), liver portal triad (HP), Bile Duct (BD), vessels (BA), interstitial tissue (BI), and Liver (LV) (mm³) in experimental groups (means±SD).[a] (p<0.05) sham *vs.* OM groups and[b] (p<0.05) OM *vs. V. arctostaphylos* treated groups.

V. arctostaphylos and OM effects on p53 and Bcl-2 positive cells

The evaluation of parameters related to apoptosis rate in liver and kidney cells revealed interesting findings. The administration of OM resulted in a significant increase ($p<0.05$) in the percentage of p53 positive cells (%) and a significant decrease ($p<0.05$) in Bcl-2 cells (%). These effects were attributed to the activation of apoptotic pathways. On the other hand, the fruit extract of *V. arctostaphylos* exhibited an opposite impact by dose-dependently reducing the percentage of p53 positive cells (%) and increasing the percentage of Bcl-2 cells (%) in the liver and kidney. These changes were particularly significant ($p<0.05$) at doses of 200 and 400 mg/kg, indicating the inhibitory effect of the extract on apoptotic pathways (Figures 7, 8 and 9).

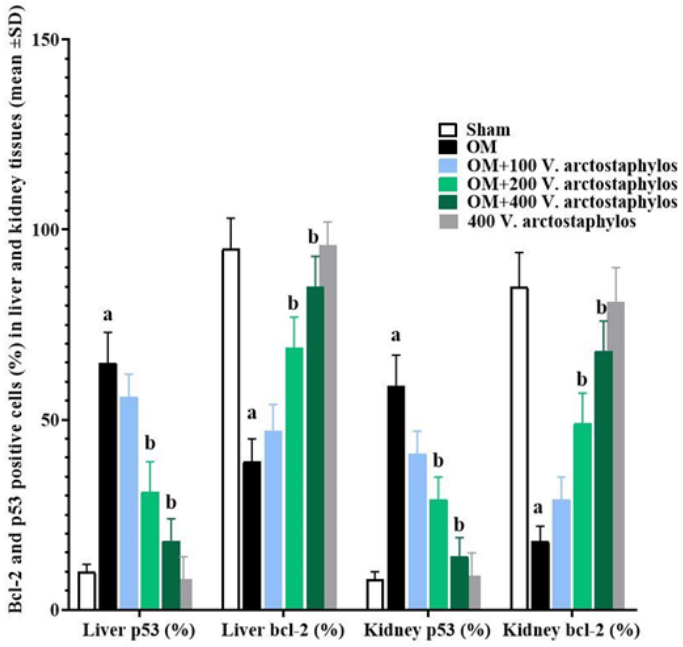

Figure 7: Bcl-2 and p53 positive cells (%) in liver and kidney tissues by immunohistochemistry in experimental groups (means±SD).[a] ($p<0.05$) sham *vs.* OM groups and[b] ($p<0.05$) OM *vs. V. arctostaphylos* treated groups.

Histopathology of liver and kidney

After evaluating the histopathology of the liver in the studied groups, it was found that OM had detrimental effects on the liver. These effects included the destruction of liver parenchyma, lymphocytic infiltration, and fibrosis. Moreover, the replacement of collagen fibers in the main parenchyma resulted in congestion and hyperemia in the vessels of the lobules' triad. Additionally, there was a noticeable loss of structural order in the dis regions, extending from the central venule to the hepatic port triad. In the groups receiving *V. arctostaphylos*, it was observed that the normal architecture of liver lobules, dis space, and linear arrangement of hepatocytes were maintained, and this effect was dose-dependent. Furthermore, there was a reduction in lymphocytic infiltration, hyperemia, edema, and congestion. Comparatively, the presence of apoptotic bodies in the liver sinuses was less pronounced in the *V. arctostaphylos*-treated groups compared to the OM group. Additionally, a decrease in collagen synthesis and fibrosis was observed, and it followed a dose-dependent pattern in the *V. arctostaphylos*-treated groups (Figures 8 and 10).

DISCUSSION

The findings of this study demonstrate that *V. arctostaphylos* effectively safeguards the liver and kidney against damage caused by OM through its antioxidant and anti-apoptotic mechanisms, thereby preserving the normal tissue structure of these organs.

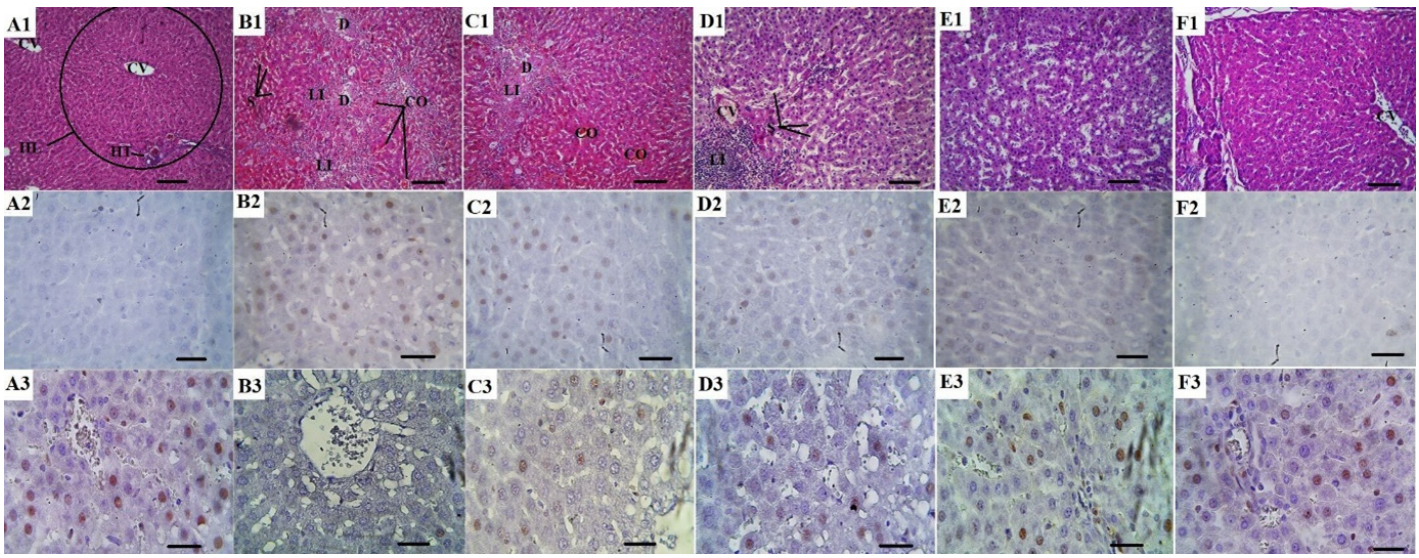

Figure 8: Histopathological and immunohistochemical findings in liver tissues in experimental groups [A1-F1 (H and E×100, scale bar=100 µm), A2-F2 (p53), and A3-F3 (bcl-2) positive cells (Immunohistochemistry×400, scale bar=25 µm)]. Congestion (CO), Lymphatic Infiltration (LI), Central Venule (CV), hepatic Degeneration (D), hepatic Sinusoid's (S), normal Hepatic Lobule (HL), and Hepatic Triad (HT).

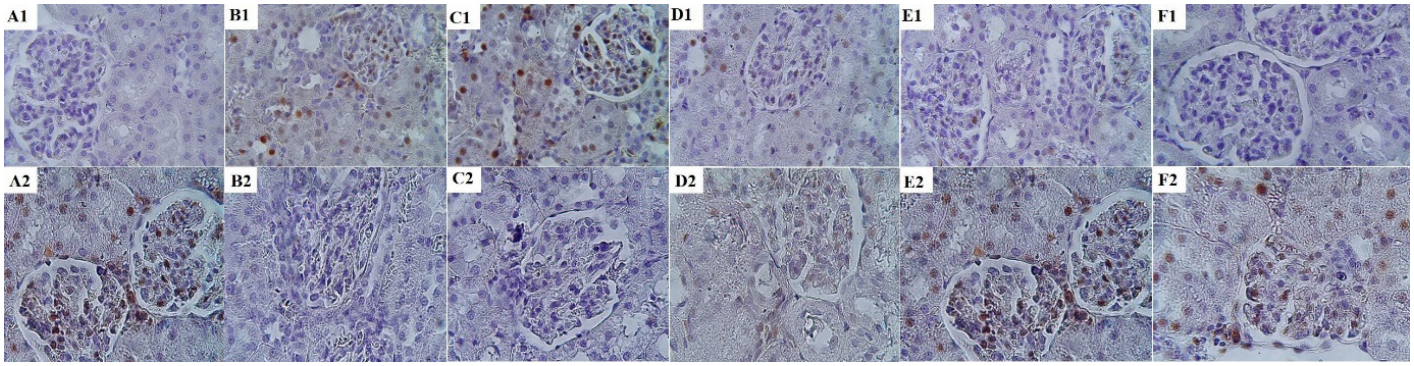

Figure 9: Immunohistochemical findings in kidney tissues in experimental groups [A1-F1 (p53×400, scale bar=100 µm) and A2-F2 (bcl-2×400, scale bar=25 µm) positive cells].

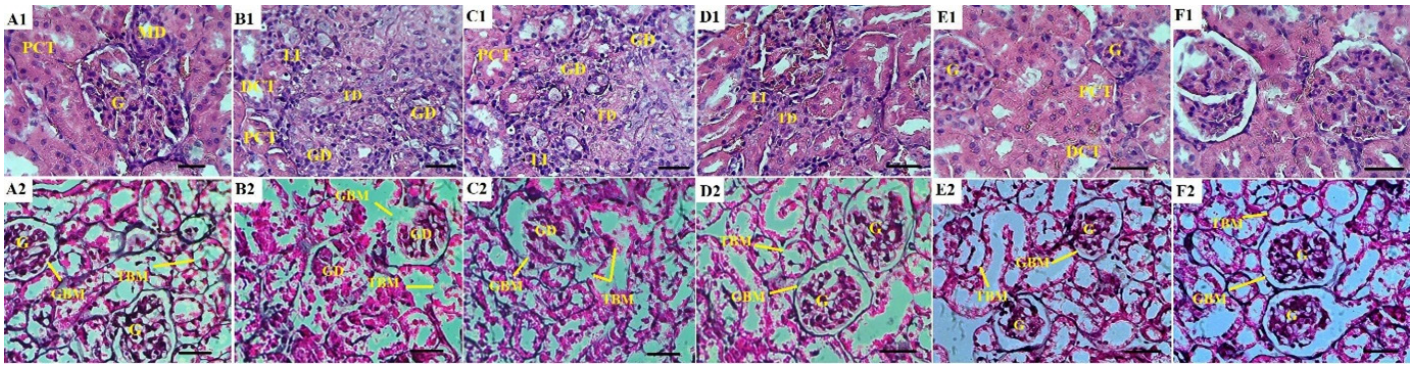

Figure 10: Histopathological findings in kidney tissues in experimental groups [A1-F1 (periodic acid–Schiff×400, scale bar=25 µm) and A2-F2 (Jones' Methenamine Silver×400, scale bar=25 µm)]. Normal glomerulus (G), Proximal Convoluted Tubule (PCT), Distal Convoluted Tubule (DCT), Blood Vessel (BV), Macula Densa (MD), lymphatic infiltration (LI), Glomerular Degeneration (GD), Tubular Degeneration (TD), Tubular Basement Membrane (TBM), and Glomerular Basement Membrane (GBM).

OM induced kidney and liver toxicity

Studies have indicated that OM can lead to pathological damage in the liver, such as cholestatic jaundice, hepatic peliosis, liver fibrosis, congestion, and edema. Furthermore, OM and its metabolites can harm the hepatocyte membrane by triggering an increase in the production of free radicals, consequently impairing normal liver function. This ultimately results in altered levels of liver functional markers. Research suggests that even therapeutic doses of OM (<5 mg/kg) can cause an elevation in serum levels of ALT, AST, ALP, and both total and direct bilirubin. Nejati *et al.* (2016) conducted a study on male NMRI mice, revealing that a dosage of 5 mg/kg/day of OM over a span of 30 days resulted in increased levels of liver enzymes (ALT, AST, ALP).[23] Similarly, Feng *et al.* (2022) demonstrated that OM-induced liver damage in rats subjected to a dosage of 5 mg/kg/day for 30 days led to elevated serum activity of ALT, AST, ALP, as well as AL and TP levels.[5] The excessive generation of ROS and Reactive Nitrogen Species (RNS) resulting from the metabolism of OM by hepatocyte cytochrome P450 and its excessive buildup in the liver and kidneys, surpassing the capabilities of the body's own antioxidant defense system, leads to harmful effects on cell membrane polyunsaturated fatty acids, protein structure, and DNA alkylation and methylation.[7] The glucuronic acid conjugates derived from ROS produced by OM and its metabolites are excreted, resulting in degradation of glomerular basement membranes, increased apoptosis of glomerular mesangial cells, reduced urinary space/Glomerular Filtration Rate (GFR), tubular basement membranes, altered cortex/medulla thickness ratio, and the formation of casts in the urinary tubules.[6] The production of ROS by OM results in their attachment to hepatocyte membranes, which subsequently leads to necrosis and membrane damage. As a consequence, the activity of AST, ALP, and ALT increases, subsequently causing the release of these enzymes into the bloodstream.[24] Studies indicate that OM induces necrosis and apoptosis of liver hepatocytes and kidney parenchymal cells by activating the signaling pathways JNK, P38, JAK, and STAT3, in addition to Bax/Bcl-2, and p53 mitochondrial apoptosis pathway.[25]

In the present study, OM (5 mg/kg) resulted in several effects. It induced the production of free radicals, leading to an increase in NO levels and a decrease in the activity of GPx and CAT. These oxidative changes triggered apoptosis and manifested through an upregulation of p53 (pro-apoptotic index) and a downregulation of Bcl-2 (anti-apoptotic index). Consequently, OM caused a disruption in the biochemical indicators (elevated liver AST, ALT and ALP enzymes, BIL levels, and increased Cr and BUN). Furthermore, stereological and histopathological evaluations

revealed that OM had necrotizing effects on the functional parenchymal structures of the liver and kidney, leading to degeneration and a decrease in their volume. These degenerative processes were accompanied by the replacement of interstitial tissues with fibrosis.

Protective effects of *V. arctostaphylos* fruit extract against OM-induced liver and kidney injury

The findings of the present study revealed several important results regarding the *V. arctostaphylos* fruit extract. The LD_{50} was determined to be 1732 mg/kg. Additionally, the extract was found to contain 229.4±10.9 mg GAE of TPC and 120.9±11.6 mg RUE Furthermore, the DPPH free radical scavenging capacity of the extract was measured at 519.1±10.1 µmol eq. Trolox/10 g dried plant, indicating its antioxidant potential. Moreover, the FRAP content was recorded at 1516.6±55.3 mmol, further highlighting its antioxidant capacity. It is worth noting that Mahboubi's *et al.* (2013) study on the fruit extract of this plant reported TPC and TFC contents of 107.9 and 5.4 mg/g, respectively.[26] Güder *et al.* (2014) conducted a study on the fruit extract of this plant and reported significant findings. They found that the extract contained a TPC of 118.67 mg/g of dry extract and a TFC of 16.87 mg/g of dry extract. Additionally, they demonstrated that this extract possesses a DPPH free radical scavenging capacity of 797.1 µmol eq. Trolox/1 g, indicating its antioxidant potential.[27] These results showed that *V. arctostaphylos* fruit extract used in this study has high polyphenol content and high antioxidant power. The study conducted by Bazm *et al.* (2018) shed light on the protective effects of *V. arctostaphylos* fruit extract on kidney function in cases of gentamicin-induced damage. The findings indicated that administering a 400 mg/kg dose of the extract led to decreased levels of BUN and Cr compared to the group that received only gentamicin.[17] Similarly, another study performed on Wistar rats to investigate the impact of *V. arctostaphylos* fruit extract on acute liver injury induced by carbon tetrachloride (CCl_4) yielded promising results. The study demonstrated that administering this plant extract effectively reduced the levels of liver enzymes in rats treated with *V. arctostaphylos*+CCl_4 compared to the CCl_4 group.[28] These findings highlight that *V. arctostaphylos* fruit extract, at doses of 200 and 400 mg/kg, holds potential in enhancing liver and kidney function by improving biochemical markers. More importantly, it promotes a harmonious balance between the generation and elimination of free radicals triggered by OM, mainly due to its high content of polyphenolic compounds. Additionally, it effectively enhances the activity of CAT and GPx, ultimately resulting in the reduction of NO levels.

Studies have indicated that *V. arctostaphylos* fruit extract, particularly its polyphenolic compounds such as Quercetin, Kaempferol, Genistein, Apigenin, and anthocyanins, exhibit protective properties for liver parenchyma cells.[29] These compounds effectively inhibit the ROS-mediated MAPKs and NF-κB pathways.[30-32] They also enhance the expression of Chk2, p53, p21, and p27. Moreover, these compounds play a crucial role in safeguarding the kidneys and preventing apoptosis induction within them.[33] Furthermore, studies have demonstrated that these compounds possess the ability to safeguard the integrity of renal tubules and glomeruli by countering oxidative damage through diverse mechanisms. These mechanisms encompass inhibiting the angiotensin-converting enzyme (ACE), restraining the Na+/K+ ATPase enzyme activity, and promoting the upregulation of aquaporin-2 channels (AQP2).[34] In the current study, it was observed that the *V. arctostaphylos* fruit extract, administered at doses of 200 and 400 mg/kg, exhibited the capacity to decrease the count of p53-positive cells while simultaneously boosting the number of Bcl-2-positive cells. This effect was achieved through the inhibition of mitochondrial apoptosis pathways. By regulating the normal cell cycle and safeguarding cells against the apoptotic cascade, the extract contributed to the preservation of tubular membrane integrity, hepatocytes, and other parenchymal cells. Consequently, there was an increase in the volume of parenchymal tissue, offering protection against necrosis, fibrosis, and interstitial tissue damage.

Although the present findings demonstrate the potential of *V. arctostaphylos* fruit extract in safeguarding the liver and kidney function and structure against oxidative damage induced by AAs, further investigations, particularly clinical trials, are needed to explore additional pathways and potential benefits.

CONCLUSION

Medicinal plants, whether in their natural form or as derived substances, contain abundant polyphenol compounds that possess notable antioxidant, anti-apoptotic, and anti-inflammatory properties. These properties enable them to effectively protect the structure and function of various tissues against the detrimental effects of anabolic steroids and their metabolites. Individuals engaged in bodybuilding, especially those using anabolic steroids, can derive substantial benefits from the protective potential offered by these plants. The findings of this study suggest that the extract derived from *V. arctostaphylos* fruit shows promise as a prodrug or supplement in the pharmaceutical industry, particularly for individuals with liver-kidney failure. However, it is advisable to conduct further research to investigate the molecular pathways and mechanisms through which this extract exerts its effects.

ACKNOWLEDGEMENT

The authors would like to thank Torbat Heydarieh University of Medical Sciences, Torbat Heydarieh, Iran, for the support of this research, which is based on a research project contract.

FUNDING

This study was approved and supported by a grant from Torbat Heydarieh University of Medical Sciences, Torbat Heydarieh, Iran (grant number: 401000021).

CONFLICT OF INTEREST

The authors declare that there is no conflict of interest.

ABBREVIATIONS

NO: Nitric oxide; **SOD:** Superoxide dismutase; **GPx:** Glutathione peroxidase; **CAT:** Catalase; **TPTZ:** 2, 4, 6-Tripyridyl-riazine; **ROS:** Reactive oxygen species; **OM:** Oxymetholone; **TNF-α:** Tumor necrosis factor-α; **IL-6:** Interlekine-6; **DCT:** Distal convoluted tubules; **PCT:** Proximal convoluted tubules; **LC-ESI/MS:** Liquid chromatography electrospray ionization mass spectrometry; **TPC:** Total phenolic content; **TFC:** Total flavonoid content; **DPPH:** 2, 2-diphenyl-1-picrylhydrazyl; **FRAP:** Ferric reducing antioxidant power; **AST:** Aspartate aminotransferase; **ALT:** Alanine aminotransferase; **ALP:** Alkaline phosphatase; **BUN:** Blood urea nitrogen; **BIL:** Bilirubin; **TP:** Total Protein; **Cr:** Creatinine; **IUR:** Isotropic uniform random; **H and E:** Hematoxylin and eosin; **PAS:** Periodic acid Schiff.

ETHICAL APPROVAL

This research adhered to ethical guidelines for the use of animal subjects. Animal welfare considerations were taken into account, minimizing pain, distress, and suffering. Ethical approval was obtained from the Torbat Heydarieh University of Medical Sciences (approval number: IR.THUMS.AEC.1401.006) for animal research.

SUMMARY

V. arctostaphylos fruit extract, rich in polyphenols and possessing antioxidant properties, can enhance protection against OM-induced hepato-renal oxidative damage.

REFERENCES

1. Khamda M, Hosseini MH, Rezaee M. Measurement and correlation solubility of cefixime trihydrate and oxymetholone in supercritical carbon dioxide (CO_2). J Supercrit Fluids. 2013; 73: 130-7. doi: 10.1016/j.supflu.2012.09.006.
2. Sobolevsky T, Rodchenkov G. Mass spectrometric description of novel oxymetholone and desoxymethyltestosterone metabolites identified in human urine and their importance for doping control. Drug Test Anal. 2012; 4(9): 682-91. doi: 10.1002/dta.1407, PMID 22945829.
3. Khan NT, Bibi M, Yousuf S, Qureshi IH, Al-Majid AM, Mesaik MA, *et al.* Synthesis of some potent immunomodulatory and anti-inflammatory metabolites by fungal transformation of anabolic steroid oxymetholone. Chem Cent J. 2012; 6(1): 1-11.
4. Akbari Bazm M, Khazaei M, Khazaei F, Naseri L. *Nasturtium officinale* L. hydroalcoholic extract improved oxymetholone-induced oxidative injury in mouse testis and sperm parameters. Andrologia. 2019; 51(7): e13294. doi: 10.1111/and.13294, PMID 31025410.
5. Feng J, Gao H, Yang L, Xie Y, El-Kenawy AE, El-kott AF. Renoprotective and hepatoprotective activity of *Lepidium draba* L. extracts on oxymetholone-induced oxidative stress in rat. J Food Biochem. 2022; 46(9): e14250. doi: 10.1111/jfbc.14250, PMID 35633194.
6. Karimi Jashni H, Bandak S, Mahjoor A. The effect of oxymetholone on the kidney tissues of one day old rats. J Med Sci. 2022; 9(3): 8-13. doi: 10.29252/jmj.9.3.2.
7. Ali ZS, Hashem LH. The pre-emptive impact of Arabic gum to antagonist the renal dysfunction, oxidative stress, and gene expression of antioxidant in kidney of rat that oxymetholone-Induced. Acta Biol Med. 2023; 94(1): e2023104.
8. Tarashande Foumani A, Elyasi F. Oxymetholone-induced acute renal failure: a case report. Caspian J Intern Med. 2018; 9(4): 410-2. doi: 10.22088/cjim.9.4.406, PMID 30510659.
9. Almaghrabi OA. Molecular and biochemical investigations on the effect of quercetin on oxidative stress induced by cisplatin in rat kidney. Saudi J Biol Sci. 2015; 22(2): 227-31. doi: 10.1016/j.sjbs.2014.12.008, PMID 25737657.
10. Bagherniya M, Nobili V, Blesso CN, Sahebkar A. Medicinal plants and bioactive natural compounds in the treatment of non-alcoholic fatty liver disease: A clinical review. Pharmacol Res. 2018; 130: 213-40. doi: 10.1016/j.phrs.2017.12.020, PMID 29287685.
11. Feshani AM, Kouhsari SM, Mohammadi S. *Vaccinium arctostaphylos*, a common herbal medicine in Iran: molecular and biochemical study of its antidiabetic effects on alloxan-diabetic Wistar rats. J Ethnopharmacol. 2011; 133(1): 67-74. doi: 10.1016/j.jep.2010.09.002, PMID 20850514.
12. Shamilov AA, Olennikov DN, Pozdnyakov DI, Bubenchikova VN, Garsiya ER, Larskii MV. Caucasian blueberry: comparative study of phenolic compounds and neuroprotective and antioxidant potential of *Vaccinium myrtillus* and *Vaccinium arctostaphylos* leaves. Life (Basel). 2022; 12(12): 2079. doi: 10.3390/life12122079, PMID 36556444.
13. Fakhri S, Iranpanah A, Gravandi MM, Moradi SZ, Ranjbari M, Majnooni MB, *et al*. Natural products attenuate PI3K/Akt/mTOR signaling pathway: A promising strategy in regulating neurodegeneration. Phytomedicine. 2021; 91: 153664. doi: 10.1016/j.phymed.2021.153664, PMID 34391082.
14. Bellavia D, Dimarco E, Costa V, Carina V, De Luca A, Raimondi L, *et al.* Flavonoids in bone erosive diseases: perspectives in osteoporosis treatment. Trends Endocrinol Metab. 2021; 32(2): 76-94. doi: 10.1016/j.tem.2020.11.007, PMID 33288387.
15. Hakimi M, Soltani R, Keshvari M, Asgari S, Sarrafzadegan N. The effects of *Vaccinium arctostaphylos* on lipid profile in mild hyperlipidemia patients-a randomized clinical trial. J Shahrekord Univ Med Sci. 2014; 16(5).
16. Akbaribazm M, Khazaei MR, Khazaei F, Khazaei M. Doxorubicin and *Trifolium pratense* L. (red clover) extract synergistically inhibits brain and lung metastases in 4T1 tumor-bearing BALB/c mice. Food Sci Nutr. 2020; 8(10): 5557-70. doi: 10.1002/fsn3.1820, PMID 33133558.
17. Bazm MA, Khazaei M, Ghanbari E, Naseri L. Protective effect of *Vaccinium arctostaphylos* L. fruit extract on gentamicin-induced nephrotoxicity in rats. Comp Clin Pathol. 2018; 27(5): 1327-34. doi: 10.1007/s00580-018-2743-0.
18. Wang Y, Bai L, Li H, Yang W, Li M. Protective effects of *Lepidium draba* L. leaves extract on testis histopathology, oxidative stress indicators, serum reproductive hormones and inflammatory signalling in oxymetholone-treated rat. Andrologia. 2021; 53(11): e14239. doi: 10.1111/and.14239, PMID 34520070.
19. Blainski A, Lopes GC, De Mello JCP. Application and analysis of the folin ciocalteu method for the determination of the total phenolic content from *Limonium brasiliense* L. Molecules. 2013; 18(6): 6852-65. doi: 10.3390/molecules18066852, PMID 23752469.
20. Davoodi F, Taheri S, Raisi A, Rajabzadeh A, Zakian A, Hablolvarid MH, *et al*. Leech therapy (*Hirudo medicinalis*) attenuates testicular damages induced by testicular ischemia/reperfusion in an animal model. BMC Vet Res. 2021; 17(1): 256. doi: 10.1186/s12917-021-02951-5, PMID 34315461.
21. Akbari M, Goodarzi N, Tavafi M. Stereological assessment of normal Persian squirrels (*Sciurus anomalus*) kidney. Anat Sci Int. 2017; 92(2): 267-74. doi: 10.1007/s12565-016-0332-3, PMID 26894271.
22. Warner JD, Irazabal MV, Krishnamurthi G, King BF, Torres VE, Erickson BJ. Supervised segmentation of polycystic kidneys: a new application for stereology data. J Digit Imaging. 2014; 27(4): 514-9. doi: 10.1007/s10278-014-9679-y, PMID 24639063.
23. Nejati V, Zahmatkesh E, Babaei M. Protective effects of royal jelly on oxymetholone-induced liver injury in mice. Iran Biomed J. 2016; 20(4): 229-34. doi: 10.7508/ibj.2016.04.007, PMID 27178489.
24. Amirkhani R, Farzaei MH, Ghanbari E, Khazaei M, Aneva I. *Cichorium intybus* improves hepatic complications induced by oxymetholone: an animal study. Journal of Medicinal plants and By-product. 2022; 11(1): 111-8.
25. Keshtmand Z, Akbaribazm M, Bagheri Y, Oliaei R. The ameliorative effects of *Lactobacillus coagulans* and *Lactobacillus casei* probiotics on CCl4-induced testicular toxicity based on biochemical, histological and molecular analyses in rat. Andrologia. 2021; 53(1): e13908. doi: 10.1111/and.13908, PMID 33225493.
26. Mahboubi M, Kazempour N, Taghizadeh M. *In vitro* antimicrobial and antioxidant activity of *Vaccinium arctostaphylos* L. extracts. J Biol Act Prod Nat. 2013; 3(4): 241-7. doi: 10.1080/22311866.2013.782696.
27. Güder A, Engİn MS, Yolcu M, Gür M. Effect of processing temperature on the Chemical Composition and Antioxidant Activity of *Vaccinium arctostaphylos* Fruit and Their Jam. J Food Process Preserv. 2014; 38(4): 1696-704. doi: 10.1111/jfpp.12132.
28. Ravan AP, Bahmani M, Ghasemi Basir HR, Salehi I, Oshaghi EA. Hepatoprotective effects of *Vaccinium arctostaphylos* against CCl4-induced acute liver injury in rats. J Basic Clin Physiol Pharmacol. 2017; 28(5): 463-71. doi: 10.1515/jbcpp-2016-0181, PMID 28467312.

29. Askaripour M, Najafipour H, Saberi S, Jafari E, Rajabi S. Daidzein mitigates oxidative stress and inflammation in the injured kidney of ovariectomized rats: AT1 and Mas receptor functions. Iran J Kidney Dis. 2022; 1(1): 32-43. PMID 35271498.
30. Zhang Y, Zhang JQ, Zhang T, Xue H, Zuo WB, Li YN, *et al.* Calycosin induces gastric cancer cell apoptosis via the ROS-mediated MAPK/STAT3/NF-κB pathway. Onco Targets Ther. 2021; 14: 2505-17. doi: 10.2147/OTT.S292388, PMID 33883905.
31. Ahmad A, Biersack B, Li Y, Kong D, Bao B, Schobert R, *et al*. Deregulation of PI3K/Akt/mTOR signaling pathways by isoflavones and its implication in cancer treatment. Anticancer agents in medicinal chemistry (formerly current medicinal chemistry-anticancer agents). 2013; 13(7): 1014-24.
32. Wang Z, Jiang X, Zhang L, Chen H. Protective effects of *Althaea officinalis* L. extract against N-diethylnitrosamine-induced hepatocellular carcinoma in male Wistar rats through antioxidative, anti-inflammatory, mitochondrial apoptosis and PI3K/Akt/mTOR signaling pathways. Food Sci Nutr. 2023; 11(8): 4756-72. doi: 10.1002/fsn3.3455, PMID 37576045.
33. Medjakovic S, Mueller M, Jungbauer A. Potential health-modulating effects of isoflavones and metabolites via activation of PPAR and AhR. Nutrients. 2010; 2(3): 241-79. doi: 10.3390/nu2030241, PMID 22254019.
34. Dong R, Pan J, Zhao G, Zhao Q, Wang S, Li N, *et al.* Antioxidant, antihyperglycemic, and anti-hyperlipidemic properties of *Chimonanthus salicifolius* SY Hu leaves in experimental animals: modulation of thioredoxin and glutathione systems, renal water reabsorption, and gut microbiota. Front Nutr. 2023; 10: 1168049. doi: 10.3389/fnut.2023.1168049, PMID 37187875.

Cite this article: Khordad E, Akbaribazm M, Hosseini SM, Rahmani Y. Protective Effects of *Vaccinium arctostaphylos* L. against Oxymetholone-Injured Liver and Kidney Injury in BALB/c Mice: An Integrated Biochemical, Stereological, Histopathological, and Immunohistochemical Study. Pharmacog Res. 2024;16(2):401-13.